Channel-Opening Kinetics of GluR2Q$_{flip}$ AMPA Receptor: A Laser−Pulse Photolysis Study†

Gang Li, Weimin Pei, and Li Niu*

Department of Chemistry and Center for Neuroscience Research, University at Albany, State University of New York, Albany, New York 12222

Received May 15, 2003; Revised Manuscript Received August 15, 2003

ABSTRACT: AMPA receptors mediate fast excitatory neurotransmission in the central nervous system. GluR2 is an AMPA receptor subunit that controls some key heteromeric AMPA receptor properties, such as calcium permeability. The kinetic properties of GluR2, relevant to the time scale of its channel opening, however, are poorly understood. Here, to measure the channel-opening kinetics, we use a laser−pulse photolysis technique, which permits glutamate to be liberated photolytically from γ-*O*-(α-carboxy-2-nitrobenzyl)glutamate (caged glutamate) with a time constant of ∼30 μs. We show that GluR2Q$_{flip}$, an unedited and Ca^{2+} permeable isoform, is by far the fastest ligand-gated channel with the channel-opening and -closing rate constants being $(8.0 \pm 0.49) \times 10^4$ and $(2.6 \pm 0.20) \times 10^3$ s^{-1}, respectively. Therefore, the shortest rise time (20−80% of the receptor current response) or the fastest observed time by which the GluR2Q$_{flip}$ channel can open is predicted to be 17 μs. The minimal kinetic mechanism for the channel opening is further consistent with the binding of two glutamate molecules with the channel-opening probability of 0.96. These results suggest that GluR2 is a temporally, highly efficient receptor to transduce the binding of chemical signals (i.e., glutamate) into an electrical impulse.

Ionotropic glutamate receptors (iGluRs)[1] are the major excitatory neurotransmitter receptor proteins in the mammalian brain (*1, 2*). As a class of membrane proteins, iGluRs are composed of domains that span the membrane to form a small pore or channel, which is gated by glutamate, a neurotransmitter. When glutamate, released from a presynaptic neuron, binds to a postsynaptic glutamate receptor, the receptor rapidly changes its conformation and transiently forms an open ion channel, thus resulting in a change of the postsynaptic membrane potential. A postsynaptic potential of sufficient strength triggers an action potential, which will in turn propagate the initial nerve impulse. The major function of iGluRs is to mediate fast synaptic neurotransmission underlying the basic activities of the brain, such as memory and learning. Overactivation of the receptors, on the other hand, has been implicated in a number of neurological diseases such as post-ischemia cell death, epilepsy, Huntington's chorea, and amyotrophic lateral sclerosis (*1*). To date, three major subtypes of iGluRs have been identified: *N*-methyl-D-aspartate (NMDA), kainate, and AMPA receptors, based on amino acid sequences, pharmacological profiles, and biological functions (*1*, *2*).

Rapid opening of a ligand-gated ion channel receptor is the key step for the receptor to convert the binding of a chemical signal (i.e., neurotransmitters or ligands) into an electrical impulse at a chemical synapse of nervous systems. Knowing the kinetic mechanism of channel opening has four main implications. First, the knowledge enables more accurate prediction of the time course of the open-channel form of the receptor as a function of neurotransmitter concentration, which determines the transmembrane voltage change and in turn controls synaptic neurotransmission. Second, the kinetic mechanism provides mechanistic clues for the rational design of compounds to regulate the receptor activity, thereby influencing the temporal activity of the synapse. Third, this work aids the investigation of functional consequences of a structural variation, relevant to the time scale of the channel opening. Finally, the characterization of the channel-opening rate constants is required to understand quantitatively the integration of nerve impulses that arrive at a single neuron or that are generated at a single neuron from different receptors responding to the same chemical signal.

Here, we first report the kinetic mechanism for the opening of the GluR2Q$_{flip}$ receptor channel, a key AMPA receptor subunit. In the companion paper, we report the results for GluR6Q, a kainate receptor subunit. We then discuss the functional implications for the two receptors, derived from the kinetic characterizations.

Despite significant advances in understanding the molecular structure and function for the GluR2 receptor (*1*−*5*), the characterization of the channel-opening kinetics remains a formidable challenge. Single-channel recording of GluR2 to measure the lifetime of the open channel has so far defied analysis (*6*). Fast solution-exchange methods have not offered a time resolution high enough to resolve the rapid channel opening, occurring in the microsecond (μs)-to-millisecond (ms) time domain, from the rapidly ensuing channel desen-

† This work was supported in part by grants to L.N. from the American Heart Association (0130513T), Amyotrophic Lateral Sclerosis Association, and Muscular Dystrophy Association. G.L. was supported by a postdoctoral fellowship from the Muscular Dystrophy Association.

* To whom correspondence should be addressed. Telephone: (518) 442-4447. Fax: (518) 442-3462. E-mail: lniu@albany.edu.

[1] Abbreviations: AMPA, α-amino-3-hydroxy-5-methyl-4-isoxazolepropionic acid; αCNB glutamate, γ-*O*-(α-carboxy-2-nitrobenzyl)-glutamate; GFP, green fluorescent protein; iGluRs, ionotropic glutamate receptors; NMDA, *N*-methyl-D-aspartate; SV40 TAg, Simian virus 40 large T-antigen.

10.1021/bi0347961 CCC: $25.00
Published on Web 10/01/2003

sitization, occurring in the ms time domain, which leads to the closure of the channel with the neurotransmitters bound.

In this study, we use a combination of two approaches to achieve a high expression of GluR2 and a high time resolution characterization. The first approach is the use of a powerful oncoprotein, Simian virus 40 (SV40) large T-antigen (TAg) (*7*), to enhance the GluR2 expression in human embryonic kidney (HEK)-293 cells. The coexpression of TAg leads to an increase of the GluR2 expression at a single-cell level by up to a factor of 5 and thus permits the recording of sizable current responses induced even at low ligand concentrations. The second approach is the use of the laser−pulse photolysis technique (*8*−*10*) to release biologically active glutamate from the biologically inert caged glutamate or γ-*O*-(α-carboxy-2-nitrobenzyl)glutamate with a time constant of ~30 μs (*11*). This technique provides a time resolution of ~60 μs and allows a kinetic characterization of the glutamate-induced channel opening prior to channel desensitization.

We choose the unedited GluR2 receptor isoform or GluR2Q in which a glutamine (Q) is present at the Q/R site (amino acid 586) in the channel-lining region (*12*). By RNA editing, the glutamine is replaced by an arginine (R) (*12*). This Q/R site is a key molecular determinant in that, for instance, AMPA receptors containing GluR2Q are highly Ca^{2+} permeable, whereas those containing GluR2R are not (*5*). It has been proposed that intracellular Ca^{2+} overload via Ca^{2+} permeable AMPA receptors is a primary mechanism leading to neurodegeneration. Moreover, changes in the GluR2 editing efficiency and in GluR2 mRNA levels (*12*) are linked to pathogenic conditions such as ischemia (*13*) and amyotrophic lateral sclerosis (*14*). Furthermore, the isoform we choose to study is the flip splice variant ($GluR2Q_{flip}$), which is known to desensitize relatively slowly and have a sizable steady-state nondesensitizing current, as compared to the flop isoform (*15*).

MATERIALS AND METHODS

Expression of cDNA and Cell Culture. The original cDNA encoding $GluR2Q_{flip}$ was kindly provided by Prof. Steve Heinemann (Salk Institute) and was cloned into the pcDNA3.1 vector (Invitrogen), which contains the SV40 origin. The plasmid was propagated in the *Escherichia coli* host (DH5α) and purified using a kit from QIAGEN (Valencia, CA). Both the HEK-293T and the HEK-293S cells were cultured in Dulbecco's modified Eagle's medium supplemented with 10% fetal bovine serum and in a 37 °C, 5% CO_2, humidified incubator. $GluR2Q_{flip}$ was transiently expressed in these cells using a calcium phosphate method (*16*). Unless otherwise noted, HEK-293 cells were also cotransfected with a plasmid coding for green fluorescent protein (GFP) and another plasmid, pRSV-TAg, for SV40 TAg. The weight ratio of the plasmids for GFP and TAg to that for GluR2 was 2:1:10, and the GluR2 used for transfection was 2−6 μg/35 mm dish. Transfected cells were allowed to grow for >48 h before use. The pRSV-TAg and GFP plasmids were generous gifts from Profs. Jeremy Nathans (Johns Hopkins University) and Ben Szaro (SUNY−Albany).

Whole-Cell Current Recording. Glutamate, a natural neurotransmitter, was used as the activating ligand, and the resulting receptor response was recorded. Recording electrodes were made from glass capillaries from World Precision Instruments (Sarasota, FL) and fire polished. The electrode resistance was ~3 MΩ when filled with the electrode solution. The electrode solution contained (in mM) 110 CsF, 30 CsCl, 4 NaCl, 0.5 $CaCl_2$, 5 EGTA, and 10 Hepes (pH 7.4 adjusted by CsOH). The external bath solution contained (in mM) 150 NaCl, 3 KCl, 1 $CaCl_2$, 1 $MgCl_2$, and 10 Hepes (pH 7.4 adjusted by NaOH). All chemicals were from commercial sources. The GFP fluorescence in cells was visualized using an Axiovert S100 microscope with a fluorescent detection system from Carl Zeiss (Thornwood, NY). The whole-cell current (*17*) was recorded using an Axopatch-200B amplifier at a cutoff frequency of 2−20 kHz by a built-in, eight-pole Bessel filter and digitized at 5−50 kHz sampling frequency using a Digidata 1322A from Axon Instruments (Union City, CA). The data acquisition software was pCLAMP 8, also from Axon Instruments.

Laser−Pulse Photolysis. The setup for the laser−pulse photolysis experiment has been described previously (*8*, *18*). αCNB glutamate, purchased from Molecular Probes (Eugene, OR), was dissolved in the external bath buffer and delivered to the cell using a cell-flow device (see next). Once a HEK-293 cell was in the whole-cell mode (*17*), it was lifted from the bottom of the dish and suspended in the external bath solution. After the cell was equilibrated with caged glutamate for 250 ms, a laser pulse was delivered to liberate free glutamate. A single laser pulse at 355 nm with a pulse length of 8 ns was generated from a Minilite II pulsed Q-switched Nd:YAG laser from Continuum (Santa Clara, CA), tuned by a third harmonic generator. The laser light was coupled into a fiber optic from FiberGuide Industries (Stirling, NJ), and the power was adjusted to be 200−800 μJ, detected by a Joulemeter from Gentec (Quebec, Canada).

To vary the concentration of the photolytically released glutamate in kinetic measurements, the power of the laser was adjusted and/or the concentration of the caged glutamate was varied. To determine the concentration of the photolytically released glutamate, at least two glutamate solutions with known concentrations were used to measure the current amplitudes on the same cell before and after a laser pulse. The free glutamate solution was delivered to the cell using the cell-flow device (see next). The current amplitudes obtained from the cell-flow measurements were compared to the amplitude from the laser measurement, with reference to the relationship of the current amplitude as a function of glutamate concentration (or the dose−response relation). These measurements were also used to monitor any damage to the receptors and/or the cell for successive experiments with the same cell.

Cell-Flow Measurements. The cell-flow device was used to deliver either caged glutamate for the laser−pulse photolysis described previously or free glutamate to monitor the cell damage and to calibrate the concentration of photolytically released glutamate (*8*, *18*). The cell-flow device consisted of a U-tube (*19*) with an aperture of ~150 μm (*18*). The linear flow rate, controlled by two peristaltic pumps, was 4 cm/s. A HEK-293 cell was placed 50−100 μm away from the U-tube aperture. The time resolution of the cell-flow method is 1.9 ± 0.5 ms (10−90% glutamate-induced current rise), obtained from the measurements of >100 cells expressing the receptor. When free glutamate was used, the amplitude of the whole-cell current was corrected for receptor desensitization during the rise time by a method previously described (*19*). The correction is necessary because the observed current amplitude depends on the rise time of the amplitude, the fraction of the open channel, and the desensitization rate constant. The method is based on hydrodynamic theories to describe fluid flowing over a spherical object, such as (by approximation) a HEK-293 cell suspended in the external bath solution. When a solution flows over a cell, the time for the ligand molecules in the solution to mix with receptors varies because of uneven flow rates of the ligands over the cell surface. By the correction method, the time course of the current is first divided into a constant time interval, and then the observed current (I_{obs}) is corrected for the desensitization that occurs during each time interval (Δt). After the current is determined for each of n constant time intervals ($n\Delta t = t_n$), the corrected, total current (I_A) is given by eq 1

$$I_A = (e^{\alpha \Delta t} - 1)\sum_{i=1}^{n}(I_{obs})\Delta t_i + (I_{obs})\Delta t_n \qquad (1)$$

where α represents the rate constant for receptor desensitization, and $(I_{obs})\Delta t_i$ is the observed current during the ith time interval. t_n is equal to or greater than the current rise time. I_A obtained from this correction method is independent of the solution velocities (an example is shown in the inset of Figure 3A). The validity of this method was demonstrated using several independent approaches (*8*, *19*). The current correction program was kindly provided by Prof. George P. Hess from Cornell University.

All measurements were performed with cells voltage-clamped at −60 mV, pH 7.4 and 22 °C. Each data point was an average of at least three measurements collected from at least three cells unless otherwise noted. Linear regression and nonlinear least-squares fitting (Levenberg−Marquardt algorithm) were performed using Origin 7 (Origin Lab, Northampton, MA). Uncertainties reported are the standard error of the fits unless noted otherwise.

RESULTS

Activation of GluR2Q$_{flip}$ by Glutamate. The glutamate-activated whole-cell response was recorded, using the cell-flow device (*19*). As seen in Figure 1A, the response increased rapidly, indicating channel opening, and then returned toward the baseline due to desensitization. In contrast, the control experiment, using nontransfected cells, showed no response even at 10 mM glutamate, a concentration that would have evoked a maximum current response for the transfected cell (see the dose−response in Figure 3A). The observed desensitization rate for the GluR2Q$_{flip}$ receptor was characterized by a first-order rate constant, which described >95% of the progression of the desensitization reaction in all the current traces. The desensitization rate constant increased with increasing glutamate concentration but eventually reached a plateau (Figure 1B). The mean value of the maximum rate constant, independent of ligand concentration, was 163 s^{-1} (time constant of 6 ms). The receptor desensitization profile and the magnitude of the rate constant at a given glutamate concentration observed in this study are consistent with those previously reported (*20*).

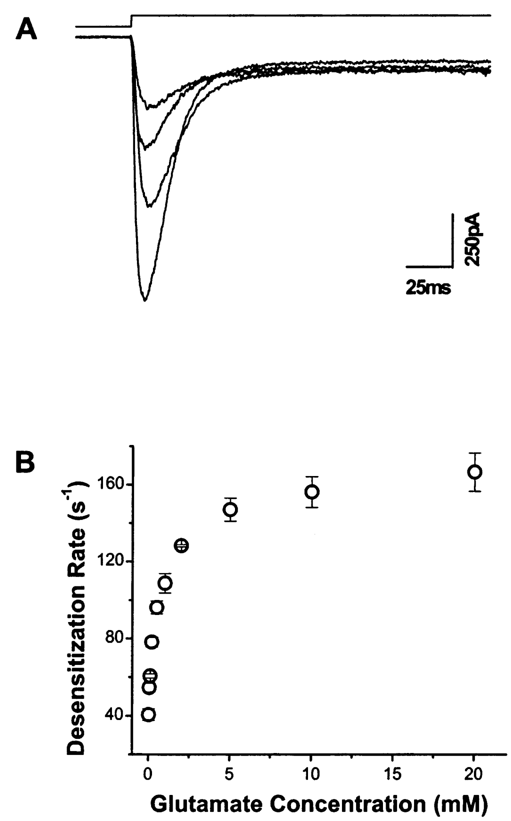

FIGURE 1: (A) Whole-cell current response to glutamate at concentrations of (from bottom up) 1000, 500, 200, and 100 μM. (B) Dependence of the desensitization rate constant on glutamate concentration. The desensitization rate was characterized by a first-order rate constant and is shown with a standard error of mean. Each data point is an average of at least three measurements from three cells.

Coexpression of GFP and TAg in HEK-293 Cells. By examining the desensitization rate constant, we evaluated whether the coexpression of both GFP and TAg in HEK-293 cells affected the kinetic properties of GluR2Q$_{flip}$ expressed in the same cell. GFP is a widely used intracellular marker because of its characteristic green fluorescent color and was used in this study to facilitate the selection of a cell that may also express GluR2 receptors for recording. TAg was used to enhance GluR2 expression (the rationale and the result are presented in detail next). We found that neither protein expressed in the same cell affected the kinetic properties of GluR2. This was evidenced, in Figure 2, by the similar relative current amplitudes and desensitization rate constants at a given glutamate concentration, which were determined from both the cells that expressed only GluR2 and those that expressed GFP and TAg additionally. In control experiments, the cells expressing GFP or TAg separately or together, but without GluR2Q$_{flip}$, yielded no response to glutamate even at a saturating concentration (i.e., 10 mM) (data not shown).

Minimal Kinetic Mechanism for Channel Opening. Figure 3A displays the dose−response relationship, established with the current amplitude corrected for receptor desensitization (see Materials and Methods) as a function of glutamate concentration. This relationship was analyzed using eq 2.

$$I_A = I_M R_M \frac{L^2}{L^2 + \Phi(L + K_1)^2} \qquad (2)$$

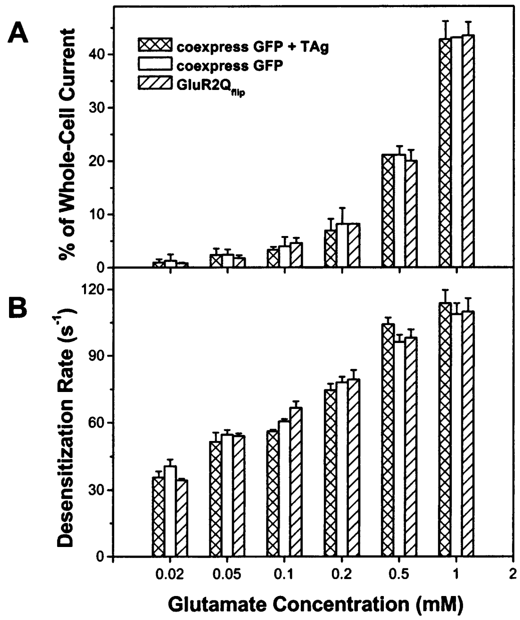

FIGURE 2: Coexpression of GFP and TAg in HEK-293 cells does not affect (A) relative current amplitudes and (B) desensitization rate constants for GluR2Q$_{flip}$ response induced by glutamate. In panel A, the whole-cell currents from different cells were normalized to the current obtained at 1 mM glutamate, and the current amplitude at 10 mM was set to be 100% (see also dose−response plot in Figure 3A).

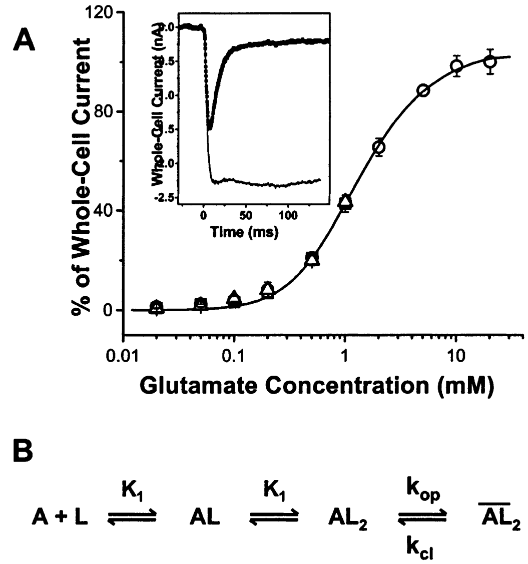

FIGURE 3: (A) Whole-cell current amplitude as a function of glutamate concentration or dose−response relationship. The square represents the measurements for the HEK-293 cells expressing only GluR2Q$_{flip}$, the circle for cells expressing both GluR2Q$_{flip}$ and GFP, and the triangle for cells expressing GluR2Q$_{flip}$, GFP, and pRSV-TAg, respectively. The observed whole-cell current was corrected for desensitization (see Materials and Methods). Shown in the inset is such an example in which the observed current amplitude is represented by solid dots, while the corrected amplitude is shown by a solid line. The whole-cell currents from different cells were normalized to the current obtained at 1 mM glutamate, and the current amplitude at 10 mM was set to be 100%. Parameters of the best fit using eq 1, shown in solid line, were K_1 of 1.27 ± 0.28 mM, Φ of 0.55 ± 0.26, and $I_M R_M$ of 164 ± 28. (B) A minimal kinetic mechanism for the channel opening of GluR2Q$_{flip}$. The mechanism involves two ligand-binding steps. A represents the active, unliganded form of the receptor, L the ligand (glutamate), AL and AL$_2$ the ligand-bound closed channel forms, and $\overline{AL_2}$ the open channel form of the receptor. Other symbols are defined in the text. For simplicity, it is assumed that glutamate binds to the two sites with equal affinity designated by K_1, the intrinsic equilibrium dissociation constant.

I_A represents the current amplitude, L the molar concentration of the ligand, I_M the current per mol of receptor, and R_M the number of mol of receptor in the cell. Φ^{-1} ($=k_{op}/k_{cl}$) is the channel-opening equilibrium constant, and K_1 is the intrinsic dissociation constant for ligand. Eq 2 was derived based on a minimal kinetic mechanism for the channel opening, shown in Figure 3B. This mechanism is general for ligand-gated ion channels including native glutamate receptors (*21*, *22*). The mechanism is consistent with the assumption that the binding of at least two glutamate molecules is required to open an AMPA receptor channel, as previously proposed (*20*, *23*). Accordingly, K_1 of 1.27 ± 0.28 mM was obtained from the best fit, using eq 2. For comparison with the reported EC$_{50}$ value (the ligand concentration that corresponds to 50% of the maximum response), the Hill equation (*24*) was further used to analyze the same dose−response data. The EC$_{50}$ of 1.32 ± 0.04 mM and the Hill coefficient of 1.3 ± 0.1 obtained are comparable with the EC$_{50}$ of 1.39 mM and the Hill coefficient of 1.08 previously reported (*20*). Furthermore, the K_1 value is qualitatively comparable with the EC$_{50}$ values. In addition, the dose−response relationship established here was also used in calibration of the concentration of the photolytically released glutamate in laser photolysis experiments (see Materials and Methods).

Characterization of Caged Glutamate with GluR2Q$_{flip}$ in HEK-293 Cells. To apply the laser−pulse photolysis technique for the kinetic measurement of the GluR2Q$_{flip}$ channel opening, the caged glutamate must fulfill several criteria (*10*, *25*). Among them, caged glutamate must be biologically inert. Furthermore, the caged glutamate should release, upon photolysis, free glutamate in the μs time region. Rapid release ensures that the photochemical uncaging rate is not limiting to the channel-opening reaction.

Previously, caged glutamate was found to liberate free glutamate with a rate constant of ~30 μs and to be biologically inert to glutamate receptors in rat hippocampal neurons (*11*), which were known to express endogenous AMPA receptors (*21*, *22*). Here, we further tested the biological properties of the caged glutamate exclusively with the GluR2Q$_{flip}$ receptor expressed in the HEK-293 cells. The glutamate-elicited receptor responses in the absence and presence of caged glutamate were found to be identical, as judged by both the current amplitude and the desensitization rate, in Figure 4. In this test, the concentration of the caged glutamate was 2 mM, the highest used in the laser experiments. This result demonstrated that the caged glutamate did not activate the GluR2Q$_{flip}$ channel, nor did it inhibit or potentiate the glutamate response.

Channel-Opening Kinetics Characterized by Laser−Pulse Photolysis. Using the laser−pulse photolysis technique with caged glutamate, we determined the rate constants for the opening of the GluR2Q$_{flip}$ channel. Figure 5A shows a representative whole-cell current response. The rising phase of the current reflects the channel-opening reaction, whereas the current fall is due to channel desensitization. A single-exponential rate law (eq 3) was adequate to describe >95% of the rising phase at all the concentrations of photolytically released glutamate, ranging from 100 to 380 μM. This observation is consistent with the assumption that the rate

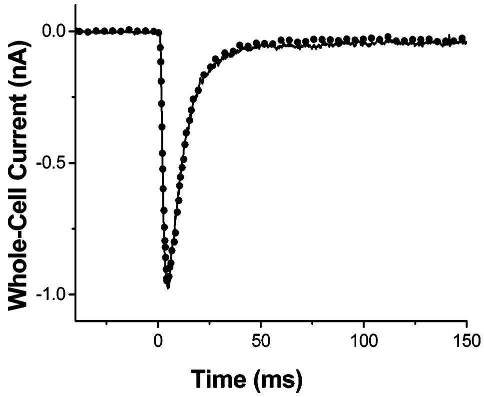

FIGURE 4: Caged glutamate is biologically inert to GluR2Q_{flip} as tested with GluR2Q_{flip} expressed in HEK-293 cells. Superimposed were the whole-cell currents induced by 200 μM glutamate in the absence (line) and presence (solid circle) of 2 mM caged glutamate. The sampling frequency was 5 kHz. For clarity, however, the number of points, shown in the solid-circle trace, was reduced in various regions of the current trace.

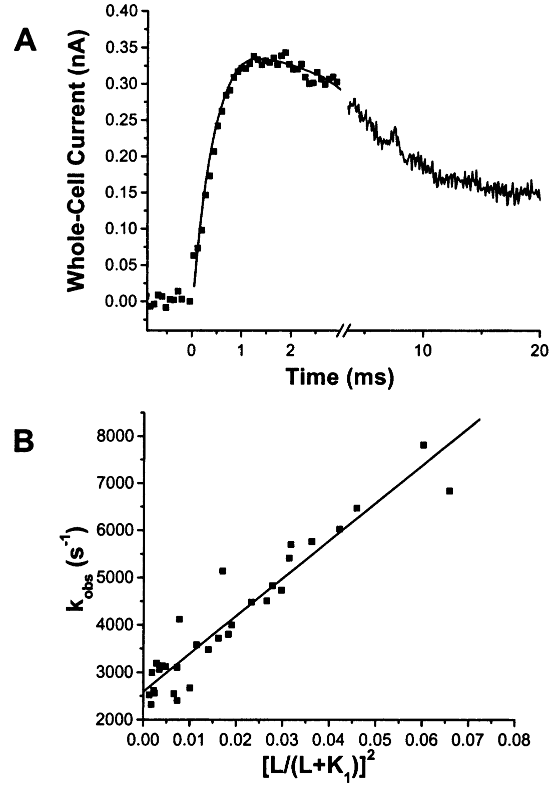

FIGURE 5: Laser−pulse photolysis measurements of the channel-opening kinetics for GluR2Q_{flip}. (A) A representative whole-cell current is shown from the opening of the GluR2Q_{flip} channel initiated by the laser−pulse photolysis of caged glutamate at time zero. (B) Plot of k_{obs} as a function of glutamate concentration by eq 4. Each point represents a k_{obs} obtained at a particular concentration of photolytically released glutamate. The k_{cl} and k_{op} were $(2.6 \pm 0.20) \times 10^3$ and $(8.0 \pm 0.49) \times 10^4$ s^{-1}, respectively. In this plot, the lowest data point chosen, corresponding to the lowest concentration of photolytically released glutamate, was 100 μM (or ~4% of the fraction of the open channel). In choosing this concentration or the fraction of the open channel, we compared the kinetic characterization of the channel opening for the muscle nicotinic acetylcholine receptor (*8*, *9*). In such a case, 20 μM carbamoylcholine, which corresponded to ~4% of the fraction of the open channel, was the concentration where the value of k_{obs} obtained in the laser−pulse photolysis measurement correlated well to that of k_{cl}. The value of k_{cl} further agreed with the lifetime of the open channel, determined independently using single-channel recording (*8*). Using the fraction of the open-channel form, rather than the absolute ligand concentration, takes into account the different ligand affinity values.

of ligand binding is fast relative to the rate of channel opening (*8*) (see the mechanism in Figure 3B and the discussion next). Accordingly, the channel-opening rate constant (k_{op}) and the channel-closing rate constant (k_{cl}) were derived from the analysis of the observed first-order rate constant (k_{obs}) as a function of ligand concentration, using eq 4.

$$I_t = I_A(1 - e^{-k_{obs}t}) \tag{3}$$

$$k_{obs} = k_{cl} + k_{op}\left(\frac{L}{L + K_1}\right)^2 \tag{4}$$

I_A is the maximum current amplitude, while I_t represents the current amplitude at time t. Eq 3 was used to calculate the k_{obs} value at a glutamate concentration. From Figure 5B, k_{cl} of $(2.6 \pm 0.20) \times 10^3$ s^{-1} and k_{op} of $(8.0 \pm 0.49) \times 10^4$ s^{-1} were obtained respectively, using eq 4.

In the derivation of eq 4 for the kinetic analysis of k_{obs} as a function of ligand concentration, we assumed that the ligand-binding rate(s) (including both the first and the second steps, in Figure 3B) was fast, relative to the rate of channel opening. The rate constant of glutamate binding to the singly and doubly liganded states is not known. However, some clues about this rate constant can be drawn from the measurement of the glutamate binding to the extracellular portion of the GluR4 receptor, known as S1S2, by Madden and co-workers (*26*). The glutamate association rate constant to the S1S2 was reported to be 1.6×10^7 M^{-1} s^{-1} at 5 °C (*26*). At room temperature, therefore, this rate constant is expected to become even larger, provided the ligand binding behaves linearly according to the Arrhenius equation. Furthermore, the foregoing assumption is supported by our experimental observation. If the observed rate constant represented the rate of the transition from the closed- to the open-channel form, as shown in Figure 3B, the rising phase of the receptor response was expected to be a single-exponential rate process and to remain so even when the concentration of the ligand varied. In our experiments, a single-first-order rate process for the rising phase of the receptor response was indeed observed in all the concentrations of the photolytically liberated glutamate. On the other hand, this result is inconsistent with the assumption that the rate of ligand-binding steps is similar to the rate of channel opening. If true, double-exponential rate processes would appear in the rising phase as the concentration of ligand is varied, because both ligand-binding and channel-opening would contribute to the kinetics. Furthermore, if the binding rate was slow, as compared to the rate of the channel opening, eq 4 would not satisfy the concentration dependence of k_{obs}.

Channel-Opening Rate Process Can Be Separated from the Channel Desensitization in the Laser−Pulse Photolysis Measurements. With an increasing concentration of glutamate, the rise time of the whole-cell current in the laser−pulse photolysis experiment became shorter, or the observed rate of the channel opening became faster (Figure 5). Concomitantly, the observed desensitization rate was also faster (Figure 1B). However, the current rise, indicative of channel opening, was always more than 10 times faster than the current fall, due to channel desensitization, as shown in Figure 5A. This was true at all the concentrations of glutamate in the laser photolysis measurements. This result demonstrates that the channel-opening reaction can be cleanly separated from the desensitization reaction. Consistent with this conclusion, simultaneous fitting of both the rising and the falling phases by two first-order rate equations yielded a k_{obs} value, which was identical (within a 5% error range) to the k_{obs} value obtained in the single fit by using eq 3. Consequently, the analysis of the channel-opening rate process involved only the rising phase of the whole-cell current (using eq 3), and the minimal mechanism for channel opening in Figure 3B upon which the kinetic analysis was based did not involve the desensitization reaction.

The kinetic mechanism we propose in Figure 3B stands in contrast to the previous kinetic model, which was based on the assumption that the desensitization is kinetically linked to channel activation (*20*). Accordingly, the rate constants pertaining to the channel-opening reaction were derived from measuring and fitting the desensitization rate process (*20*). As a result, the channel-opening rate constant obtained by fitting (*20*) is 5-fold lower, while the channel-closing rate constant is ~2-fold higher, as compared to the values obtained from the present study.

Although the minimal mechanism we propose for the kinetic characterization of the channel-opening process does not involve desensitization, we do not argue against the involvement of the desensitization reaction that may begin when ligand binds, as previously proposed (*20*, *27*). We argue, however, that the desensitization reaction does not occur appreciably during the rise time of the channel opening. This argument is based on our results that the observed channel-opening rate constant is much larger than the observed channel-desensitization rate constant at any given glutamate concentration. Therefore, the channel-opening rate process can be measured effectively as a kinetically distinct, separable rate process from the slower desensitization rate that only becomes dominant in a longer time scale. Jin et al. (*28*) recently proposed that the GluR2 receptor channel, once opened after binding to glutamate, preferentially returns to the ground state without entering the desensitization state. This conclusion was based on the ratio of $k_{off}/k_{des} = 15$ (rate of the channel closure after ligand removal vs rate of the receptor desensitization) for glutamate, as compared to 2.2 for quisqualate whose binding to the receptor preferentially leads to the desensitization state.

Enhancement of GluR2Q$_{flip}$ Expression in HEK-293 Cells by TAg. To enhance the expression of GluR2 at a single-cell level, we coexpressed an oncoprotein, SV40 TAg, with GluR2 in the HEK-293 cells. We found that the GluR2Q$_{flip}$ expression at the level of a single HEK-293S cell could be enhanced up to a factor of 5 on average, as illustrated in Figure 6, and to a lesser degree in the HEK-293T cells. Here, the current response, as an assay at a given concentration of ligand, was proportional to the number of receptor molecules expressed on the cell surface (see eq 2). The enhancement of GluR2Q$_{flip}$ expression by TAg was likely due to its transforming activity by which the binding of TAg to key tumor suppressors such as p53 and the cell cycle regulatory proteins such as retinoblastoma family proteins (pRBs) inactivates the functions of these proteins (*7*). TAg coexpression has been successfully used previously, for instance, to enhance the expression of recombinant rhodopsin (*29*).

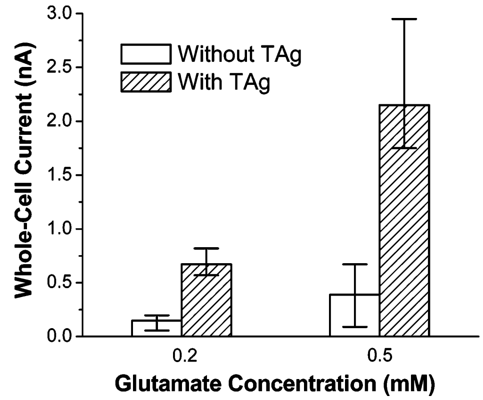

FIGURE 6: Enhancement of GluR2Q$_{flip}$ expression by TAg in HEK-293S cells as detected by whole-cell recording. At 0.2 mM glutamate concentration, a total of 42 cells without the coexpression of TAg and 68 cells with TAg were sampled, respectively. At 0.5 mM glutamate concentration, 43 cells without TAg and another 43 cells with TAg were measured, respectively. The height of each column indicates the average response from 80% of the cells sampled. The height of each bar represents the range of the current observed for 80% of the cells. However, we did not test the cells containing GluR2Q$_{flip}$ and TAg at glutamate concentrations higher than 1 mM because the receptor currents in the presence of TAg were often too large to be accurately measured using the Axopatch-200B amplifier.

The necessity to enhance the GluR2 receptor expression at a single-cell level was apparent for the following reasons. The GluR2 expression in the HEK-293 cells is generally not as high as compared to other AMPA receptor subunits (*15*). In one report, the GluR2Q$_{flip}$ receptor response was detectable only when a high concentration of glutamate was used (*30*). Further, in measuring the lifetime of the open channel or k_{cl}, the ligand concentration used should be kept low (see eq 4: $k_{obs} = k_{cl}$ when $L \ll K_1$), thus potentially making the current response, proportional to the number of receptor channels to be bound and opened with ligand, too low to be detected. For example, Swanson et al. (*6*) previously attempted but were unable to observe single-channel events with the GluR2Q receptor. Sun et al. (*4*), on the other hand, showed some sizable GluR2Q receptor responses, but a high concentration of glutamate was used. In addition, GluR2Q$_{flip}$ has a much higher EC_{50} value than other AMPA receptor subunits (*1*). Consequently, glutamate at a low concentration, such as 100 μM, induces an even smaller receptor current. As shown in the present study, the coexpression of TAg in the HEK-293 cells yielded a significant increase of the GluR2Q$_{flip}$ expression in the HEK-293 cells. The enhancement of the receptor response at a single-cell level has made it more feasible for the laser–pulse photolysis measurements.

DISCUSSION

In the present study, we have characterized the kinetic mechanism for the opening of the GluR2Q$_{flip}$ channel. To achieve this, we combined two approaches involving a rapid kinetic technique with a high time resolution (~60 μs) and an enhanced expression method using an oncoprotein TAg in HEK-293 cells.

The magnitude of k_{op} is a measure of how fast the GluR2Q$_{flip}$ channel can open following the binding of glutamate. The k_{op} of 80 000 s^{-1} or the equivalent $t_{1/2}$ of about

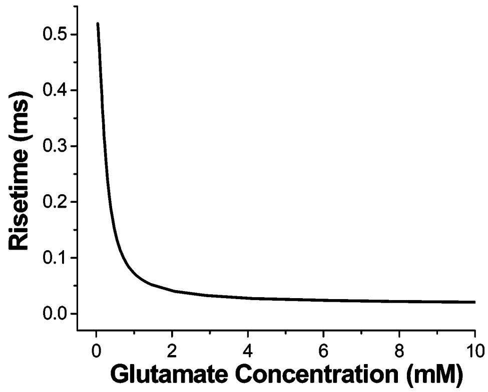

FIGURE 7: Rise time for the opening of the GluR2Q_{flip} channel. The rise time is defined as the time for the receptor current response to rise from the 20 to the 80% level (see Figure 5A) and is obtained by converting a k_{obs} value by a first-order rate equation. The relationship of the k_{obs} with the glutamate concentration was established using the experimentally determined k_{op} and k_{cl} as shown in eq 4.

10 μs points to a μs time scale for the opening of the channel in response to the binding of glutamate. If the channel opening is assumed to be linked to the lobe closure as suggested by Gouaux and Armstrong (*31*), the k_{op} then reflects the rate of lobe closure. In this model, the β-sheet core of lobe 2 of the S1S2 (the extracellular ligand-binding domain of GluR2) forms part of the ligand-binding pocket. Measurements of amide bond dynamics by NMR spectroscopy suggest that residues within this region undergo motions in the μs time scale (*32*). Thus, concerted motions on the μs time scale that lead to channel opening are feasible. The value of k_{cl}, on the other hand, reflects how fast the open channel closes or indicates the lifetime of the open channel ($k_{cl} = 1/\tau$, τ is the lifetime). The k_{cl} of 2600 s^{-1} suggests that the mean lifetime for the open channel is about 0.4 ms. Previously, neither the channel-opening rate constant nor the lifetime of the open channel has been experimentally determined (see Note Added in Proof).

The characterization of the k_{cl} and k_{op} for the GluR2Q_{flip} receptor further allows us to establish the time course by which the GluR2Q_{flip} channel operates as a function of glutamate concentration. If the rise time is used to represent the time course of the opening of the channel, then the rise time is expected to decrease with increasing the ligand concentration. For GluR2Q_{flip}, this can be readily illustrated by using eq 4 with the experimentally measured k_{cl} and k_{op} values. The conversion of a k_{obs} value to the corresponding rise time by a first-order rate law is displayed in Figure 7 (the rise time is defined as the time for the receptor current response to rise from the 20 to the 80% level).

There are several features worth noting in Figure 7. First, this figure predicts a quantitative relationship for the dependence of the rise time on the concentration of glutamate. The relationship takes into account both the channel-closing rate constant and the affinity of glutamate to the receptor (i.e., K_1 value). However, this prediction is based on the assumption that the rate of glutamate binding is faster than that of the channel opening. The supporting evidence came from the experimental observation that a single-exponential rate process accounted for over 95% of the rising phase, shown in Figure 5A, at all the concentrations of glutamate in the laser−pulse photolysis experiments. We note, however, that when the ligand concentration becomes very low, the assumption stated above is no longer tenable. The k_{obs} value will then reflect the binding rate of the ligand rather than a relationship as described in eq 4. Under this circumstance, the rise time may be less sensitive to the change of ligand concentration, which has been previously observed with the muscle nicotinic acetylcholine receptor (*33*). Second, the rise time becomes invariant when the glutamate concentration reaches 10 mM or higher. This can be rationalized by eq 4 in that when $L \gg K_1$, k_{obs} becomes the maximum. Under this condition, k_{obs} is no longer dependent on the concentration of ligand since the receptor is saturated by bound glutamate. Consequently, the channel can open within the shortest rise time, ~17 μs, which also represents the fastest observed time by which the GluR2Q_{flip} channel can open. Third, the maximum k_{obs} can be, in fact, estimated by k_{op} alone since $k_{op} \gg k_{cl}$.

Since the channel-opening and -closing rate constants were determined, the channel-opening probability (P_{op}) or the probability by which the channel can open, once bound with ligands (*34*), can be calculated. P_{op} in this case is 0.96 [$P_{op} = k_{op}/(k_{op} + k_{cl})$]. The P_{op} of 0.96 represents that the channel-opening rate constant is ~30 times larger than the channel-closing rate constant, suggesting that the channel opening, induced by the binding of glutamate, is highly favorable. It is interesting to note, however, that GluR2Q_{flip} has a high K_1 or EC_{50} value as compared to other channels (*1*).

Our results further elucidate the time scale by which GluR2Q_{flip} operates in comparison to other known ligand-gated channels, including glutamate receptor channels. Table 1 provides a summary of known channel-opening and -closing rate constants for glutamate receptors (*35*−*37*), as compared to the corresponding values of GluR2Q_{flip}. It should be noted that some of the values listed came from the experimental measurements of the channel opening in the absence of channel desensitization, whereas some were derived by fitting the deactivation/desensitization reactions. As seen, the k_{op} of 8.0×10^4 s^{-1} is the largest rate constant among the glutamate receptor channels. Furthermore, this value is nearly 1 order of magnitude larger than the k_{op} for the muscle nicotinic acetylcholine receptor from BC3H1 cells (*8*) and the slowly desensitizing $GABA_A$ (γ-aminobutyric acid) receptor (*38*). Notably, the adult mouse muscle nicotinic acetylcholine receptor ($\alpha_2\beta\delta\epsilon$) has a channel-opening rate constant of 50 000 s^{-1} (*39*), which comes close to the k_{op} value of GluR2Q_{flip}. The GluR2Q_{flip} is thus by far the fastest ligand-gated channel to open upon ligand binding. On the other hand, the k_{cl} of 2600 s^{-1} for GluR2Q_{flip} suggests that this is also a fast channel to close, as compared to other ligand-gated ion channels (*8*, *21*, *38*, *39*), including the glutamate-activated AMPA receptors in hippocampal neurons (k_{cl} = 1100 s^{-1}) (*21*) (see also Table 1). These results therefore suggest that GluR2Q_{flip} has a high temporal efficiency to convert the binding of a chemical signal to an electrical impulse, although the duration of the open channel as a measure of the receptor activity is transient.

If the channel properties of GluR2Q_{flip} provide a glimpse of how the AMPA receptor functions, then at least one of the potential functions could be conceived. The ability of GluR2Q_{flip} to rapidly open and close, coupled with the probability of the channel opening being near unity, may enable the AMPA receptor to rapidly depolarize the mem-

Table 1: Channel-Opening and -Closing Rate Constants for Glutamate Receptors

glutamate receptor type (source)	k_{op} (s^{-1})	k_{cl} (s^{-1})	technique	ref
$GluR2Q_{flip}$ (HEK-293 cells)	8.0×10^4	2.6×10^3	laser−pulse photolysis	present paper
NMDA (NR1a/NR2A) (*Xenopus* oocytes)	77	28	single-channel recording	*35*
$GluR1_{flip}$ (HEK-293 cells)	7.0×10^3	2.6×10^3	fitting from rapid glutamate flow	*37*
AMPA receptors (hippocampal neurons)	9.5×10^3	1.1×10^3	laser−pulse photolysis	*21*
$GluR2Q_{flip}$ (*Xenopus* oocytes)	1.5×10^4	3.0×10^2	fitting from rapid glutamate flow	*20*
GluR6Q (HEK-293 cells)	1.1×10^4	4.2×10^2	laser−pulse photolysis	companion paper

[a] In all data cited, glutamate is the activating ligand. An average mean duration time is cited in single-channel data.

brane potential so as to quickly relieve the putative Mg^{2+} block of the NMDA receptors since NMDA and AMPA receptors often colocalize at central synapses (*2*). It has been suggested that the maturation of the glutamatergic synapse and the development of synaptic plasticity require the incorporation of AMPA receptors at pure NMDA synapses, also called silent synapses (*40*, *41*). In the full activation of these synapses, the rapid opening of the AMPA channels is presumed to precede the opening of the NMDA receptors. Consistent with this hypothesis, the k_{op} of $GluR2Q_{flip}$ is 3−4 orders of magnitude larger than the k_{op} value of the NMDA receptors (*35*, *36*). Therefore, our results show the kinetic feasibility for activation of the colocalized NMDA receptors.

We have demonstrated that in the laser−pulse photolysis measurements, the channel-opening rate process, as reflected by the rising phase of the whole-cell current (μs to ms), can be measured as an elementary rate process prior to channel desensitization that occurs in a longer time scale (ms). In contrast, in the solution-exchange measurements, the rising phase observed is often mixed with channel desensitization. Therefore, the laser−pulse photolysis technique is a useful means to characterize channel-opening kinetics by measuring the desensitization-free, macroscopic current with a sufficient time resolution. This technique may be particularly useful for receptor channels that are difficult to study by single-channel recordings, due to rapid channel desensitization and low and/or multiple, complex single-channel conductance events. For instance, GluR2Q has been explored by the single-channel recording (*6*), but no fruitful results have yet been reported.

We have also demonstrated that the coexpression of oncoprotein TAg can significantly enhance the expression of $GluR2Q_{flip}$ in HEK-293 cells. This result alone has several potential applications. For instance, the effect of an inhibitor can now be investigated despite that the current responses will be reduced as the concentration of the inhibitor is increased (*9*). Further, when membrane patches are used, as routinely in the piezoelectrical perfusion technique to achieve a shorter rise time, the receptor response is adversely reduced by at least several hundred times as compared to the response from an entire cell. Coexpressing TAg may be also beneficial in this application. Finally, the combination of the high time resolution provided by the laser−pulse photolysis technique and the high expression of the $GluR2Q_{flip}$ receptor aided by coexpressing TAg should prove general for the investigation of other recombinant ligand-gated channels.

NOTE ADDED IN PROOF

Jin et al. (*42*) recently published glutamate-activated single-channel data for $GluR2Q_{flip}$. The major component (86%) of the open-channel distribution has a lifetime of 0.32 ms, which corresponds to a rate constant of 3100 s^{-1}. This value is roughly comparable to the k_{cl} of 2600 s^{-1} reported in the present study.

ACKNOWLEDGMENT

We thank Drs. Steve F. Heinemann (Salk Institute) for the $GluR2Q_{flip}$ cDNA, Jeremy Nathans (Johns Hopkins University) for the pRSV-TAg plasmid, Ben Szaro (SUNY−Albany) for the GFP construct, George P. Hess (Cornell University) for the current correction program, and Gobind Khorana (MIT) for the HEK-293S cells. We thank Drs. Eric Gouaux, Robert E. Oswald, John T. Schmidt, and Ben Szaro for critical comments on the manuscript. We are grateful to Drs. Jong M. Kim and Phil Reeves for helpful discussions.

REFERENCES

1. Dingledine, R., Borges, K., Bowie, D., and Traynelis, S. F. (1999) *Pharmacol. Rev. 51*, 7−61.
2. Hollmann, M., and Heinemann, S. (1994) *Annu. Rev. Neurosci. 17*, 31−108.
3. Armstrong, N., Sun, Y., Chen, G. Q., and Gouaux, E. (1998) *Nature 395*, 913−7.
4. Sun, Y., Olson, R., Horning, M., Armstrong, N., Mayer, M., and Gouaux, E. (2002) *Nature 417*, 245−53.
5. Lomeli, H., Mosbacher, J., Melcher, T., Hoger, T., Geiger, J. R., Kuner, T., Monyer, H., Higuchi, M., Bach, A., and Seeburg, P. H. (1994) *Science 266*, 1709−13.
6. Swanson, G. T., Kamboj, S. K., and Cull-Candy, S. G. (1997) *J. Neurosci. 17*, 58−69.
7. Ali, S. H., and DeCaprio, J. A. (2001) *Semin. Cancer Biol. 11*, 15−23.
8. Matsubara, N., Billington, A. P., and Hess, G. P. (1992) *Biochemistry 31*, 5507−14.
9. Niu, L., and Hess, G. P. (1993) *Biochemistry 32*, 3831−5.
10. Hess, G. P., and Grewer, C. (1998) *Methods Enzymol. 291*, 443−73.
11. Wieboldt, R., Gee, K. R., Niu, L., Ramesh, D., Carpenter, B. K., and Hess, G. P. (1994) *Proc. Natl. Acad. Sci. U.S.A. 91*, 8752−6.
12. Sommer, B., Kohler, M., Sprengel, R., and Seeburg, P. H. (1991) *Cell 67*, 11−9.
13. Pellegrini-Giampietro, D. E., Zukin, R. S., Bennett, M. V., Cho, S., and Pulsinelli, W. A. (1992) *Proc. Natl. Acad. Sci. U.S.A. 89*, 10499−503.
14. Takuma, H., Kwak, S., Yoshizawa, T., and Kanazawa, I. (1999) *Ann. Neurol. 46*, 806−15.

15. Mosbacher, J., Schoepfer, R., Monyer, H., Burnashev, N., Seeburg, P. H., and Ruppersberg, J. P. (1994) *Science 266*, 1059−62.
16. Chen, C., and Okayama, H. (1987) *Mol. Cell Biol. 7*, 2745−52.
17. Hamill, O. P., Marty, A., Neher, E., Sakmann, B., and Sigworth, F. J. (1981) *Pflugers Arch. 391*, 85−100.
18. Niu, L., Grewer, C., and Hess, G. P. (1996) *Chemical kinetic investigations of neurotransmitter receptors on a cell surface in a microsecond time region*, Vol. VII, Acadamic Press, New York.
19. Udgaonkar, J. B., and Hess, G. P. (1987) *Proc. Natl. Acad. Sci. U.S.A. 84*, 8758−62.
20. Koike, M., Tsukada, S., Tsuzuki, K., Kijima, H., and Ozawa, S. (2000) *J. Neurosci. 20*, 2166−74.
21. Li, H., Nowak, L. M., Gee, K. R., and Hess, G. P. (2002) *Biochemistry 41*, 4753−9.
22. Jayaraman, V. (1998) *Biochemistry 37*, 16735−40.
23. Clements, J. D., Feltz, A., Sahara, Y., and Westbrook, G. L. (1998) *J. Neurosci. 18*, 119−27.
24. Loftfield, R. B., and Eigner, E. A. (1969) *Science 164*, 305−8.
25. Niu, L., Vazquez, R. W., Nagel, G., Friedrich, T., Bamberg, E., Oswald, R. E., and Hess, G. P. (1996) *Proc. Natl. Acad. Sci. U.S.A. 93*, 12964−8.
26. Abele, R., Keinanen, K., and Madden, D. R. (2000) *J. Biol. Chem. 275*, 21355−63.
27. Trussell, L. O., and Fischbach, G. D. (1989) *Neuron 3*, 209−18.
28. Jin, R., Horning, M., Mayer, M. L., and Gouaux, E. (2002) *Biochemistry 41*, 15635−43.
29. Nathans, J. (1990) *Biochemistry 29*, 9746−52.
30. Miu, P., Jarvie, K. R., Radhakrishnan, V., Gates, M. R., Ogden, A., Ornstein, P. L., Zarrinmayeh, H., Ho, K., Peters, D., Grabell, J., Gupta, A., Zimmerman, D. M., and Bleakman, D. (2001) *Neuropharmacology 40*, 976−83.
31. Armstrong, N., and Gouaux, E. (2000) *Neuron 28*, 165−81.
32. McFeeters, R. L., and Oswald, R. E. (2002) *Biochemistry 41*, 10472−81.
33. Franke, C., Hatt, H., Parnas, H., and Dudel, J. (1991) *Biophys. J. 60*, 1008−16.
34. Sigworth, F. J. (1980) *J. Physiol. 307*, 97−129.
35. Wyllie, D. J., Behe, P., and Colquhoun, D. (1998) *J. Physiol. 510*, 1−18.
36. Zhang, Y., and Auerbach, A. (1995) *J. Neurophysiol. 74*, 153−61.
37. Robert, A., Irizarry, S. N., Hughes, T. E., and Howe, J. R. (2001) *J. Neurosci. 21*, 5574−86.
38. Jayaraman, V., Thiran, S., and Hess, G. P. (1999) *Biochemistry 38*, 11372−8.
39. Grosman, C., and Auerbach, A. (2001) *Proc. Natl. Acad. Sci. U.S.A. 98*, 14102−7.
40. Petralia, R. S., Esteban, J. A., Wang, Y. X., Partridge, J. G., Zhao, H. M., Wenthold, R. J., and Malinow, R. (1999) *Nat. Neurosci. 2*, 31−6.
41. Liao, D., Zhang, X., O'Brien, R., Ehlers, M. D., and Huganir, R. L. (1999) *Nat. Neurosci. 2*, 37−43.
42. Jin, R., Banke, T. G., Mayer, M. L., Traynelis, S. F., and Gouaux, E. (2003) *Nat. Neurosci. 6*, 803−10.

BI0347961